

Rovibrational states of ClHCl^- isotopologues up to high J : a joint theoretical and spectroscopic investigation†

Cite this: *Phys. Chem. Chem. Phys.*, 2013, **15**, 6737

Peter Sebald,^{†a} Rainer Oswald,^a Peter Botschwina^{*a} and Kentarou Kawaguchi^b

Explicitly correlated coupled cluster theory at the CCSD(T*)-F12b level (T. B. Adler, G. Knizia, and H.-J. Werner, *J. Chem. Phys.*, 2007, **127**, 221106) and two precise spectroscopic parameters (K. Kawaguchi, *J. Chem. Phys.*, 1988, **88**, 4186) were used to construct an accurate near-equilibrium analytical potential energy function (PEF) for the highly anharmonic centrosymmetric hydrogen-bonded complex ClHCl^- ($R_e = 3.1153 \text{ \AA}$). From variational calculations with that PEF, a large number of rovibrational energies of different isotopologues up to high values of the rotational quantum number J was obtained. Theory helped with the assignment of lines observed by IR diode laser spectroscopy in the $\nu_1 + \nu_3$ combination band of $^{35}\text{ClH}^{35}\text{Cl}^-$ and $^{37}\text{ClH}^{35}\text{Cl}^-$ and enabled us to elucidate rather subtle patterns of rovibrational interactions. Furthermore, transition dipole moments were predicted and analysed as well as unusual isotopic effects.

Received 27th November 2012,
Accepted 14th March 2013

DOI: 10.1039/c3cp44236e

www.rsc.org/pccp

1. Introduction

The hydrogen bichloride ion (ClHCl^-) may be considered as a prototype of a highly anharmonic hydrogen-bonded system with a large dissociation energy. Together with the very strongly bound anion FHF^- , it is rather unique due to the fact that both species and some of their isotopologues could be investigated by high-resolution diode laser infrared (IR) spectroscopy.^{1–4} While a larger number of bands was observed and analysed for FHF^- and FDF^- ,^{1–3} precise spectroscopic information on ClHCl^- isotopologues is more limited. Published line positions are restricted to the ν_3 bands (proton stretching vibration) of $^{35}\text{ClH}^{35}\text{Cl}^-$ and $^{37}\text{ClH}^{35}\text{Cl}^-$, which were observed by Kawaguchi in the range $692\text{--}724 \text{ cm}^{-1}$.⁴ For the most abundant isotopologue $^{35}\text{ClH}^{35}\text{Cl}^-$, the band origin was determined to be $\nu_3 = 722.8965(2) \text{ cm}^{-1}$. There were indications of Coriolis interaction between the ν_3 and ν_2 states and an approximate treatment allowed Kawaguchi to estimate the proton bending vibrational wavenumber as $\nu_2 = 792 \pm 9 \text{ cm}^{-1}$. As was noted in his paper, many weaker spectral lines were also detected in the 978 cm^{-1} region and

attributed to the combination band $\nu_1 + \nu_3$, with ν_1 denoting the heavy-atom stretching vibration, but no detailed analysis has been published so far. Likewise, theoretical work on the spectroscopic properties of this highly anharmonic species is still scarce. Almost simultaneously with the spectroscopic work, Botschwina and coworkers⁵ reported a two-dimensional (2D) study of the collinear potential energy surface (PES) of ClHCl^- , computed by the coupled electron pair approximation (CEPA)⁶ and a rather flexible basis set of 121 contracted Gaussian-type orbitals. Using that PES in variational calculations with a stretch-only vibrational Hamiltonian, wavenumbers and transition dipole moments for various stretching vibrational transitions of $^{35}\text{ClH}^{35}\text{Cl}^-$ and $^{35}\text{ClD}^{35}\text{Cl}^-$ were calculated. In particular, large transition dipole moments of 1.333 and 0.822 D were predicted for the ν_3 fundamental and the $\nu_1 + \nu_3$ combination band of $^{35}\text{ClH}^{35}\text{Cl}^-$, the band origins of which were calculated to be 768 and 1031 cm^{-1} , respectively. One year later, Ikuta *et al.*⁷ used Møller–Plesset (MP) perturbation theory at second and fourth orders in conjunction with a moderately large basis set of DZ + (d,p) quality to carry out a very approximate 1D and 2D analysis of the stretching vibrations of ClHCl^- and ClDCl^- . In 1991, computed rovibrational energy levels of three different isotopologues of ClHCl^- were published by Špirko *et al.*⁸ The two three-dimensional (3D) PESs employed were either based on their own calculations using many-body perturbation theory at fourth order (termed PES I) or a combination with the previous stretch-only CEPA PES⁵ (termed PES II). In the calculation of rovibrational energies, an

^a Institute of Physical Chemistry, University of Göttingen, Tammannstraße 6, D-37077 Göttingen, Germany. E-mail: pbotschw@gwdg.de; Fax: +49 551 39-3144; Tel: +49 551 39-3133

^b Department of Chemistry, Okayama University, Tsushimanaka 3-1-1, Okayama 700-8530, Japan

† Electronic supplementary information (ESI) available. See DOI: 10.1039/c3cp44236e

‡ Permanent address: Madenburgstraße 14, D-76865 Insheim, Germany.

approximate rovibrational Hamiltonian was employed which neglects part of the vibrational angular momentum and the Coriolis-type contributions. Calculations with PES II yielded $\nu_3 = 694.4 \text{ cm}^{-1}$, $\nu_2 = 789.1 \text{ cm}^{-1}$, and $\nu_1 + \nu_3 = 941.8 \text{ cm}^{-1}$, in reasonably good agreement with the above experimental values. More recently, another 2D study was published by Del Bene and Jordan.⁹ At the highest level, the underlying electronic structure calculations were carried out by the standard coupled cluster method CCSD(T),¹⁰ using the Dunning-type aug-cc-pVTZ basis set^{11–13} in slightly reduced form. For the wavenumbers of the stretching fundamentals, $\nu_1 = 308 \text{ cm}^{-1}$ and $\nu_3 = 776 \text{ cm}^{-1}$ were calculated. In 2008, an empirically corrected near-equilibrium 3D PES based on MP2 calculations with the aug-cc-pVQZ basis set^{11–13} was used by Sebald¹⁴ to calculate anharmonic vibrational wavenumbers and a number of spectroscopic constants for $^{35}\text{ClH}^{35}\text{Cl}^-$, $^{37}\text{ClH}^{35}\text{Cl}^-$, and $^{37}\text{ClH}^{37}\text{Cl}^-$. The wavenumber of the proton bending vibration was predicted to be $\nu_2 (^{35}\text{ClH}^{35}\text{Cl}^-) = 799.1 \text{ cm}^{-1}$, well within the uncertainty of the experimental estimate.⁴ Particular emphasis in Sebald's paper was given to a thorough discussion of the unusual l -type doubling constants computed for the three isotopologues of the hydrogen bichloride ion.

The present paper is devoted to a joint spectroscopic and theoretical investigation of low-lying rovibrational states of different isotopologues of ClHCl^- . On the experimental side, a detailed analysis of the combination band $\nu_1 + \nu_3$ of $^{35}\text{ClH}^{35}\text{Cl}^-$ and $^{37}\text{ClH}^{35}\text{Cl}^-$ has been carried out and will be presented here. The theoretical part deals with an extensive study of various rovibrational states of ClHCl^- and its isotopologues up to high values of the rotational quantum number J . Since current quantum-chemical calculations are not yet able to faithfully deliver rovibrational energies of such species with an accuracy of 1 cm^{-1} or better, we make use of precise spectroscopic information to slightly improve an already quite accurate *ab initio* near-equilibrium potential energy surface (PES). The PES is based on calculations by explicitly correlated coupled cluster theory involving non-linear correlation factors (see, e.g., ref. 15–18 for recent reviews). That theory leads to much more rapid convergence of the correlation energies compared to the corresponding standard theory. Of particular interest to the present work is the Coriolis interaction between the proton stretching and the proton bending vibration. An approximate analysis of that interacting system ν_3/ν_2 was already made in ref. 4, but a more extensive treatment is clearly desirable.

2. Experimental

The infrared diode laser spectrometer (ref. 19), equipped with a modification for discharge modulation, was used for the measurement of ClHCl^- spectra as described in detail in ref. 4. Briefly, the anion was produced by an AC discharge in a mixture of CHCl_3 (13.3 Pa), H_2 (2.66 Pa), and He (4 Pa). The peak-to-level current was 200 mA at 3.5 kHz. The observed line positions were calibrated using the CD_3F spectrum as standard. An example of observed spectra, displaying lines within the $\nu_1 + \nu_3$ combination bands of $^{35}\text{ClH}^{35}\text{Cl}^-$ and $^{37}\text{ClH}^{35}\text{Cl}^-$, is shown in

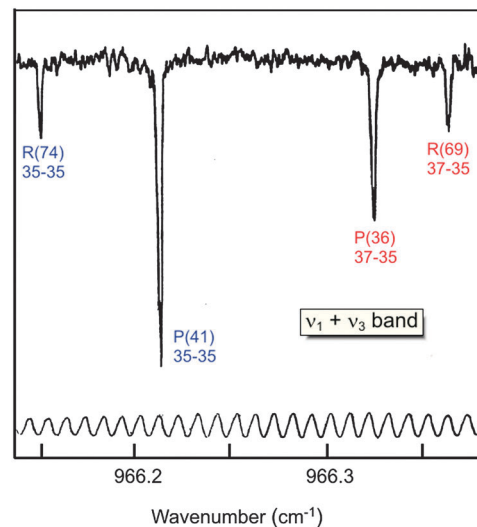


Fig. 1 Some observed lines within the $\nu_1 + \nu_3$ bands of $^{35}\text{ClH}^{35}\text{Cl}^-$ and $^{37}\text{ClH}^{35}\text{Cl}^-$.

Fig. 1, where fringes of a vacuum spaced etalon are also shown in the lower part of the figure. Over the whole wavenumber range scanned ($955\text{--}990 \text{ cm}^{-1}$, with many mode gaps), 45 lines could be assigned to $^{35}\text{ClH}^{35}\text{Cl}^-$ and 41 lines to $^{37}\text{ClH}^{35}\text{Cl}^-$. The assignments are based on the previous experimental work⁴ and were facilitated by the theoretical study of the present paper. The ground state combination difference analysis has been performed. The observed line positions are reported in Table 1 along with the differences $\nu_{\text{obs}} - \nu_{\text{calc}}$, where the calculated wavenumbers result from a fit of the rotational energy levels by means of the formula $F_v(J) = B_v J(J+1) - D_v J^2(J+1)^2$, where the collective index v stands for (ν_1, ν_2, ν_3) , with l denoting the (approximate) quantum number of the vibrational angular momentum. In contrast to the previous fits for the ν_3 bands of the two isotopologues,⁴ it was not necessary to include the sextic centrifugal distortion constant H_v which would give rise to a term of power $J^3(J+1)^3$. That issue is discussed later in comparison with the theoretical results.

Spectroscopic constants for $^{35}\text{ClH}^{35}\text{Cl}^-$ and $^{37}\text{ClH}^{35}\text{Cl}^-$ are listed in Table 2, where the data for the ν_3 state and the vibrational ground-state were taken from ref. 4. The band origin for the main isotopic species is determined to be $\nu_1 + \nu_3 = 983.2645(2) \text{ cm}^{-1}$. The gas-phase value is slightly lower than the IR absorptions at 992.6 and 1001.0 cm^{-1} that were assigned to ClHCl^- in a neon matrix-isolation study, codepositing a $\text{Ne}:\text{HCl}$ sample at 5 K with a beam of microwave excited neon atoms.²⁰ For comparison, earlier argon-matrix experiments by Milligan and Jacox²¹ yielded a lower value of 956.0 cm^{-1} , illustrating the sensitivity of the IR spectrum of ClHCl^- to the environment (see ref. 20 for more details).

Changes in the rotational constants B_v between vibrational states $\nu_1 + \nu_3$ and ν_3 amount to only 0.5%. On the other hand, the quartic centrifugal distortion constants (D_v) within the $\nu_1 + \nu_3$ state are much closer to their ground-state counterparts than to those of the ν_3 state. As we will see later from theoretical simulations, the D_v values of the ν_3 states depend

Table 1 The observed $\nu_1 + \nu_3$ bands of $^{35}\text{ClH}^{35}\text{Cl}^-$ and $^{37}\text{ClH}^{35}\text{Cl}^-$ (cm^{-1})

Line	ν_{obs}	δ^a	Line	ν_{obs}	δ^a
$(^{35}\text{ClH}^{35}\text{Cl}^-)$			$(^{37}\text{ClH}^{35}\text{Cl}^-)$		
P (49)	960.7293	2	P (45)	960.7698	1
P (48)	961.4548	-2	P (44)	961.4318	5
P (45)	963.5665	5	P (40)	963.9710	10
P (44)	964.2473	-1	P (39)	964.5778	1
P (43)	964.9169	-8	P (36)	966.3362	-1
P (41)	966.2250	1	P (31)	969.0517	-4
P (36)	969.2986	0	P (30)	969.5628	-2
P (35)	969.8799	0	P (28)	970.5526	-1
P (34)	970.4512	8	P (27)	971.0313	-1
P (33)	971.0094	-2	P (26)	971.5000	6
P (32)	971.5576	-2	P (25)	971.9566	0
P (31)	972.0944	-5	P (24)	972.4026	-6
P (30)	972.6205	-5	P (9)	977.8151	-3
P (19)	977.6772	-3	P (8)	978.0910	5
P (18)	978.0705	-4	P (6)	978.6078	-9
P (17)	978.4529	-4	R (69)	966.3740	1
P (16)	978.8240	-6	R (43)	977.6076	0
P (15)	979.1855	7	R (42)	977.8918	-2
P (14)	979.5342	2	R (41)	978.1648	-7
P (13)	979.8729	7	R (40)	978.4274	-8
P (11)	980.5164	9	R (39)	978.6792	-8
P (10)	980.8208	2	R (38)	978.9208	-1
P (9)	981.1147	1	R (37)	979.1512	2
R (41)	981.4453	-8	R (36)	979.3703	0
R (42)	981.1635	-1	R (35)	979.5783	-5
R (43)	980.8699	1	R (34)	979.7762	-2
R (44)	980.5655	6	R (33)	979.9634	2
R (45)	980.2484	-3	R (32)	980.1397	5
R (46)	979.9220	7	R (31)	980.3040	-3
R (47)	979.5825	-1	R (30)	980.4588	1
R (48)	979.2328	1	R (29)	980.6029	7
R (49)	978.8712	-4	R (28)	980.7353	3
R (50)	978.4986	-6	R (27)	980.8571	1
R (51)	978.1150	-5	R (26)	980.9687	5
R (63)	972.6294	-2	R (25)	981.0692	6
R (64)	972.0978	-9	R (23)	981.2371	1
R (65)	971.5576	12	R (22)	981.3049	-2
R (66)	971.0038	12	R (21)	981.3622	-3
R (67)	970.4384	9	R (20)	981.4085	-5
R (68)	969.8612	2	R (19)	981.4453	5
R (69)	969.2732	2	R (18)	981.4700	2
R (74)	966.1607	-6			
R (76)	964.8357	-5			
R (77)	964.1561	-3			
R (81)	961.3216	-1			

$$^a \delta = (\nu_{\text{obs}} - \nu_{\text{calc}}) \times 10^4.$$

Table 2 Spectroscopic constants of $^{35}\text{ClH}^{35}\text{Cl}^-$ and $^{37}\text{ClH}^{35}\text{Cl}^-$ (cm^{-1})^a

Constant	$\nu_1 + \nu_3$ State (this work)	ν_3 State ^b	Ground state ^b
$^{35}\text{ClH}^{35}\text{Cl}^-$			
B_v	0.09184802 (15)	0.0923147 (33)	0.0973669 (33)
$D_v \times 10^7$	0.44717 (24)	0.2450 (73)	0.3903 (66)
$H_v \times 10^{12}$		-0.97 (35)	
ν_0	983.2645 (2)	722.8965 (2)	
$^{37}\text{ClH}^{35}\text{Cl}^-$			
B_v	0.08938853 (21)	0.0898370 (37)	0.0947432 (32)
$D_v \times 10^7$	0.42833 (45)	0.2370 (82)	0.3749 (68)
$H_v \times 10^{12}$		-0.97 (65)	
ν_0	979.9062 (2)	722.9589 (2)	

^a Values in parentheses denote one standard deviation and apply to the last digits of the constants. ^b Ref. 4.

very sensitively on the choice of rotational energy levels employed in their determination.

3. Potential energy and electric dipole moment functions

Explicitly correlated coupled cluster theory at the CCSD(T*)-F12b level^{22,23} was used in the electronic structure calculations of the present work. The star denotes that the contributions from connected triple substitutions were scaled according to the recipe of Werner and coworkers.^{23,24} The atomic orbital (AO) basis set chosen for chlorine is the aug-cc-pV(5 + d)Z set,²⁵ which is combined with the aug-cc-pV5Z set for hydrogen. Both are termed AV5Z for brevity. In total, the AO basis set for ClHCl⁻ comprises 352 contracted Gaussian-type orbitals (cGTOs). Following the recommendations of Yousaf and Peterson,²⁶ the additional basis sets are chosen to be AV5Z/OPTRI, V5Z/JKFIT,²⁷ and AV5Z/MP2FIT.²⁸ Geminal exponents of $\beta = 1.4 a_0^{-1}$ ($a_0 \approx 0.5291772 \times 10^{-10}$ m) were employed as suggested by Peterson *et al.*²⁹ The 16 valence electrons were correlated in the CCSD(T*)-F12b calculations which were carried out with the MOLPRO system of *ab initio* programs.³⁰ Computations of that sort yield results very close to the basis set limit (BSL) so that consideration of the basis set superposition error and BSL extrapolation are not considered to be necessary.

According to the previous spectroscopic⁴ and theoretical work,^{5,7-9} ClHCl⁻ has a centrosymmetric linear equilibrium structure that is characterized by the single geometric parameter r_e (Cl-H equilibrium distance). Using CCSD(T*)-F12b in conjunction with the AV5Z basis set, r_e was calculated to be 1.55940 Å, with a total energy of $V_e = -920.2541389 E_h$ ($E_h \approx 4.35974394 \times 10^{-18}$ J). Analogous calculations for HCl (at $r_e = 1.27622$ Å) and Cl⁻ yield total energies of $-460.3766790 E_h$ and $-459.8402219 E_h$, respectively, so that the equilibrium dissociation energy D_e of ClHCl⁻ for fragmentation into Cl⁻ + HCl amounts to $0.0372380 E_h$ or 8172.8 cm^{-1} . We have also carried out standard CCSD(T) calculations with the large aug-cc-pCV6Z basis set which comprises 775 cGTOs in the case of ClHCl⁻ ($r_e = 1.55691$ Å, $V_e = -920.9609051 E_h$). Except for the 1s electrons of the chlorine atoms, all electrons were correlated in those calculations. At this level of theory, D_e is obtained to be 8186.3 cm^{-1} , only 0.17% higher than the above CCSD(T*)-F12b value.

In order to construct a near-equilibrium PES for ClHCl⁻, 1057 symmetry-unique energy points were calculated by CCSD(T*)-F12b/AV5Z, with relative energies of up to $10\,000 \text{ cm}^{-1}$ above equilibrium. Thereby, the energetic range of interest to the spectroscopic part of the present work, extending up to vibrational state (4,0⁰,1) at *ca.* 3000 cm^{-1} , is recovered well. After some tests we decided to set up an analytical potential energy function (PEF) as a polynomial expansion in symmetry coordinates which are equivalent to those employed by Špirko *et al.*:⁸

$$V - V_e = \sum_{ijk} C_{ijk} S_1^i S_2^j S_3^k \quad j \text{ and } k : \text{even} \quad (1)$$

In eqn (1), the symmetry coordinates S_1 – S_3 are defined as follows:

$$S_1 = \frac{1}{\sqrt{2}}(R - 2r_e) \quad (2a)$$

$$S_2 = \frac{2}{r_e}x \quad (2b)$$

$$S_3 = \sqrt{2}z \quad (2c)$$

In eqn (2a–c), R is the instantaneous distance between the two chlorine nuclei, z describes the elongation of the proton out of its equilibrium position along the Cl–Cl axis, and x measures the perpendicular distance of the proton from that axis. Weighted least-squares fitting was employed to determine the linear parameters C_{ijk} , with the weight per energy point E_i chosen to be $w_i = 1/(E_i + 750 \text{ cm}^{-1})$.² A fit with 361 parameters led to a standard deviation of 1.09 cm^{-1} . 153 of those coefficients turned out to be smaller than 10^{-6} a.u. and were neglected. The neglect has very little influence on the energies in the region of interest. Using the reduced fit (208 coefficients), all *ab initio* energy points up to 3000 cm^{-1} above the energy minimum are reproduced with a standard deviation of 0.6 cm^{-1} .

The *ab initio* PEF was empirically improved by making use of two precise experimental data for $^{35}\text{ClH}^{35}\text{Cl}^-$,⁴ the ground-state rotational constant (B_{000}) and the band origin of the proton-stretching vibration (ν_3). Two parameters, r_e and a scaling factor for symmetry coordinate S_3 , were adjusted to those experimental data by means of rovibrational calculations up to $J = 10$. The experimental values were reproduced by changing the equilibrium bond length to $r_e = 1.55766 \text{ \AA}$ and scaling S_3 with a factor of 1.00072727 . The small change in r_e (0.00174 \AA or 0.1%) and the tiny deviation of the scaling factor from unity are indications that the uncorrected PEF is already of high quality. Since the definition of S_2 depends on r_e , all relevant coefficients C_{ijk} were scaled with a factor of $(1.55766/1.55940)^j$. The 208 linear parameters of the resulting empirically corrected PEF are provided in the ESI† (Table S1), along with some further details. Some impression of the near-equilibrium PES of ClHCl^- is given by Fig. 2, which shows contour lines of relative energies in the zx -plane for four different values of the heavy-atom distance R . The characteristic development of a double-minimum potential upon increase in R is clearly obvious as is the strong coupling between coordinates z and x .

The calculation of transition dipole moments and IR intensities requires the knowledge of the variation of the electric dipole moment vector $\vec{\mu}$ with the nuclear coordinates. In the vicinity of the equilibrium structure, the electric dipole moment function (EDMF) of ClHCl^- is much simpler than its PEF, and we have decided to represent it analytically in the same way as in our previous applications to AH_2 molecules.^{31–33} Individual values for $\vec{\mu}$ were calculated by the finite field technique (field strength: 0.0003 a.u.) at 175 symmetry-unique nuclear configurations and were then transformed to the molecular Eckart frame. Subsequently, the resulting values of

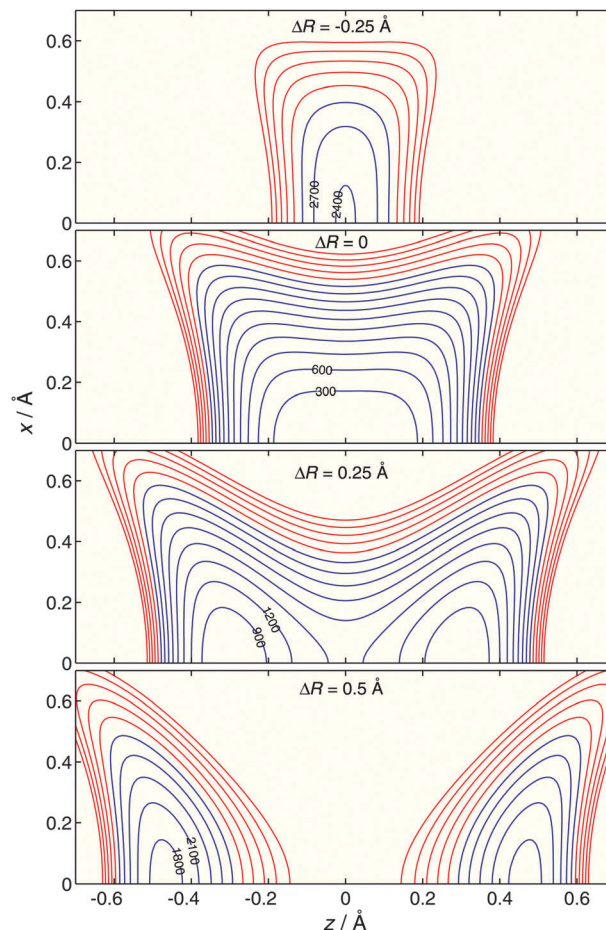


Fig. 2 Two-dimensional contour-plots of the potential energy function for ClHCl^- . Contour lines in intervals of 300 cm^{-1} with zero at the absolute energy minimum. Contour lines above 3000 cm^{-1} are drawn in red (see the text).

the parallel and perpendicular components (μ^{\parallel} and μ^{\perp}) were fitted to the expression

$$\mu^{\alpha} = \sum_{ijk} D_{ijk}^{\alpha} \tilde{S}_1^i \tilde{S}_3^j \theta^k \quad \alpha : \text{parallel or perpendicular} \quad (3)$$

In eqn (3), the coordinates \tilde{S}_1 and \tilde{S}_3 are defined as follows:

$$\tilde{S}_1 = \frac{1}{\sqrt{2}}(r_1 + r_2 - 2r_e) \text{ and } \tilde{S}_3 = \frac{1}{\sqrt{2}}(r_1 - r_2) \quad (4)$$

Here, r_1 and r_2 are the proton-chlorine distances. For a linear arrangement of the nuclei, the coordinate \tilde{S}_1 is identical to S_1 of eqn (2a) and the coordinate \tilde{S}_3 to S_3 of eqn (2c). The coordinate θ measures the deviation of the ClHCl angle from linearity. As is shown in Fig. 3, the parallel component of the electric dipole moment at $\theta = 0^\circ$ varies strongly only with the proton stretching coordinate \tilde{S}_3 and that variation is almost linear for $\tilde{S}_3 \leq 0.5 a_0$. On the other hand, μ_{\perp} changes only slightly with the angle θ ; even for a large value of $\theta = 60^\circ$, only a small value of $\mu_{\perp} \approx 0.1 e a_0$ is computed.

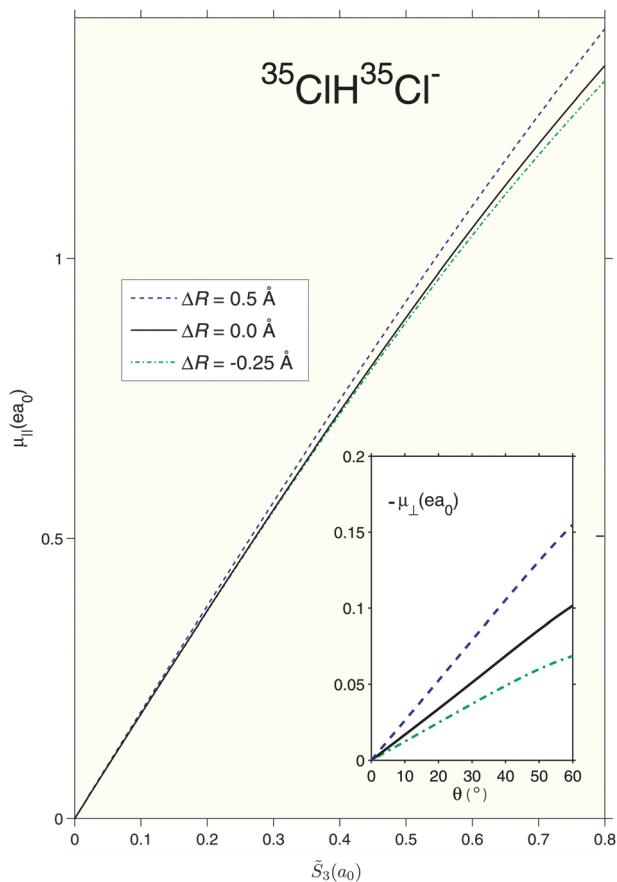


Fig. 3 Variation of the electric dipole moment of $^{35}\text{ClH}^{35}\text{Cl}^-$ with the anti-symmetric stretching coordinate \tilde{S}_3 and the angle θ (deviation from linearity).

4. Rovibrational states and their interaction

4.1. Details of calculations

The calculation of rovibrational energies and wave functions for ClHCl^- isotopologues is based on Watson's isomorphous Hamiltonian for linear molecules, which is represented in normal coordinates Q_k and the corresponding conjugate momenta P_k .³⁴ For a linear triatomic species with four vibrational degrees of freedom it may be written as follows:

$$\hat{H} = \frac{1}{2} \sum_{k=1}^4 P_k^2 + \frac{1}{2} \mu (\pi_x^2 + \pi_y^2) + \frac{1}{2} \mu (\Pi_x'^2 + \Pi_y'^2) - \mu (\Pi_x' \pi_x + \Pi_y' \pi_y) + V \quad (5)$$

The first two terms of \hat{H} constitute the vibrational kinetic energy part of the Hamiltonian, termed \hat{H}_{vib} , the third the rotational contribution (\hat{H}_{rot}) and the fourth the Coriolis part (\hat{H}_{cor}). As usual, the potential energy is denoted by V . For ClHCl^- isotopologues, the second term is rather insignificant. For the low-lying vibrational states of interest to the present work its maximum contribution to the vibrational term energies does not exceed 0.3 cm^{-1} .

The matrix elements of \hat{H} were calculated in a basis of products of symmetrized harmonic oscillator/rigid rotor

(HO/RR) functions. Specifically, one-dimensional HO functions were used for the stretching vibrations (ν_1 and ν_3) whereas two-dimensional HO functions (TDHOs) with quantum numbers ν_2 and l were employed for the bending vibration (ν_2). Integration over normal coordinates was performed by Gauss–Hermite and Gauss–Laguerre integration as suggested by Whitehead and Handy,³⁵ while integration over the Euler angles was performed analytically.³⁶ For the symmetric isotopologue $^{35}\text{ClH}^{35}\text{Cl}^-$, the vibrational basis set (for $J = 0$) was carefully selected and comprises 1136 HO products. A comparable vibrational basis of 2272 HO products was chosen for the asymmetric isotopologues. Although the present work deals with rovibrational states up to $J = 130$, we may well restrict the choice of TDHOs to relatively low l values. In our calculations for ClHCl^- isotopologues, the maximum value is chosen to be $l_{\text{max}} = 15$. Since $\nu_2 \geq l$ and the harmonic wavenumber ω_2 ($^{35}\text{ClH}^{35}\text{Cl}^-$) is as high as 828 cm^{-1} , the diagonal matrix element $\langle 0, 15^{15}, 0 | \hat{H} | 0, 15^{15}, 0 \rangle$ has an energy of almost 12000 cm^{-1} above the vibrational ground state. The influence of such a basis function on the low-lying vibrational states of interest here (stretch-only vibrational states and states with $\nu_2 = 1$) is vanishingly small and basis functions with higher l values may thus be neglected. With the given choice of l_{max} , the maximum number of HO/RR basis functions is 18 176 for symmetric and 36 352 for asymmetric isotopologues.

Squared transition dipole moments μ_{if}^2 between initial rovibrational state i and final state f were calculated from the rovibrational wavefunctions and the EDMF of Table S2 (ESI[†]), closely following the detailed description of ref. 37. They are conveniently written as the product of three factors:

$$\mu_{if}^2 \approx F_{\text{HL}} F_{\text{HW}} \mu_{\text{vv}}^2 \quad (6)$$

In eqn (6), μ_{vv} is the transition dipole moment of the pure vibrational transition, F_{HL} the Hönl–London factor,³⁶ and F_{HW} the Herman–Wallis factor.³⁸ For F_{HW} an expression of the form $(1 + A_1 m)^2$ was used with $m = -J$ and $m = J + 1$ for P-branch and R-branch transitions, respectively.³⁹ Throughout this paper, transition dipole moments are quoted in convenient units of debye ($1 \text{ D} \approx 3.33564 \times 10^{-30} \text{ C m}$).

4.2. Vibrational ground state and pure stretching vibrational states of H isotopologues

We start with those vibrational states for which direct experimental information has become available through diode laser IR absorption spectroscopy.⁴ These are the ground vibrational state $(0,0^0,0)$ and the stretching vibrational states $(0,0^0,1)$ and $(1,0^0,1)$. Calculated rovibrational term energies for the isotopologues $^{35}\text{ClH}^{35}\text{Cl}^-$, $^{37}\text{ClH}^{35}\text{Cl}^-$, and $^{37}\text{ClH}^{37}\text{Cl}^-$ up to $J_{\text{max}} = 110$ are listed in Table S3, ESI[†]. The zero-point energies of the three species are 1347.72 , 1345.36 , and 1342.95 cm^{-1} . Effective spectroscopic constants were calculated within each vibrational state $\{v\}$ by a least-squares fit with the common power expansion in $J(J + 1)$, producing B_v , D_v , (and H_v) along with the band origins (ν_3 and $\nu_1 + \nu_3$). Results of a variety of fits, differing in J_{max} and the choice of the fitting parameters, are

listed in Table 3 for $^{35}\text{ClH}^{35}\text{Cl}^-$ and $^{37}\text{ClH}^{35}\text{Cl}^-$, experimental results from Table 2 being included as well.

For the vibrational ground state, fits including the parameters B_{000} and D_{000} and with choice of $J_{\text{max}} = 10, 30, 50$, or 70 yield the rotational constant stable within 10^{-6} cm^{-1} and lead to changes in D_{000} of less than 10^{-10} cm^{-1} . Inclusion of the H_{000} term at $J_{\text{max}} = 90$ and 110 leads to tiny values for this constant and produces insignificant changes in B_{000} and D_{000} . Owing to the chosen PEF adjustment, theoretical and experimental B_{000} values for $^{35}\text{ClH}^{35}\text{Cl}^-$ are identical and the difference in B_{000} ($^{37}\text{ClH}^{35}\text{Cl}^-$) is within experimental uncertainty. The same holds for the quartic centrifugal distortion constant D_{000} of both isotopologues. The situation for the first excited state of the proton stretching vibration ($0,0^0,1$) is rather different. In this case, D_{001} depends strongly on J_{max} when the fit is restricted to B_{001} and D_{001} terms, varying between $0.2434 \times 10^{-7} \text{ cm}^{-1}$ for $J_{\text{max}} = 10$ and $0.3842 \times 10^{-7} \text{ cm}^{-1}$ for $J_{\text{max}} = 110$ (for $^{35}\text{ClH}^{35}\text{Cl}^-$). As was recognized by Kawaguchi,⁴ Coriolis interaction with the higher-lying bending vibrational state ($0,1^1,0$) may be responsible for that behavior. We will address this issue in detail in Section 4.4. Despite the high sensitivity of

D_{001} and H_{001} , agreement between theory and experiment is quite good, provided that exactly the same rovibrational transitions are included in the fits. The theoretical values for the ($0,0^0,1$) states of $^{35}\text{ClH}^{35}\text{Cl}^-$ and $^{37}\text{ClH}^{35}\text{Cl}^-$, determined as described in footnote d of Table 3, agree with experiment within 9% for D_{001} and within 16% for H_{001} , *i.e.*, the latter well within the large standard deviations of the experimental values.

Somewhat surprisingly, fits of rotational levels within the ($1,0^0,1$) state without inclusion of the H_{101} term show excellent performance up to $J_{\text{max}} = 110$, leading to very stable values for both the rotational constant and the quartic centrifugal distortion constant of both isotopologues. As we will see in Section 4.4, theory will provide an explanation for that behavior which is in line with the available spectroscopic data (*cf.* Section 2). Using the same rovibrational transitions as in the analysis of the observed lines, values for B_{101} and D_{101} are obtained that differ from the experimental values by only -0.05% and less than 2% , respectively.

The band origin of the ν_3 band of $^{37}\text{ClH}^{35}\text{Cl}^-$ is calculated to be 722.96 cm^{-1} , larger than the corresponding value of the most abundant isotopologue by 0.060 cm^{-1} (*exp.*:⁴ 0.062 cm^{-1}).

Table 3 Effective spectroscopic constants (in cm^{-1}) of $^{35}\text{ClH}^{35}\text{Cl}^-$ and $^{37}\text{ClH}^{35}\text{Cl}^-$

State	J_{max}	$^{35}\text{ClH}^{35}\text{Cl}^-^a$			$^{37}\text{ClH}^{35}\text{Cl}^-^b$		
		B_v	$D_v (\times 10^7)$	$H_v (\times 10^{12})$	B_v	$D_v (\times 10^7)$	$H_v (\times 10^{12})$
$(0,0^0,0)$	10	0.097367	0.3975		0.094740	0.3762	
	30	0.097367	0.3976		0.094740	0.3763	
	50	0.097367	0.3980		0.094740	0.3767	
	70	0.097368	0.3985		0.094740	0.3771	
	90	0.097368	0.3993		0.094740	0.3778	
		0.097367	0.3974	-0.017	0.094740	0.3761	-0.015
	110	0.097369	0.4003		0.094741	0.3787	
		0.097367	0.3972	-0.018	0.094740	0.3760	-0.016
		0.097368	0.3984		0.094742	0.3804	
	Exp. ^c	0.097367(3)	0.3903(66)		0.094743(4)	0.3749(68)	
$(0,0^0,1)$	10	0.092281	0.2434		0.089801	0.2365	
	30	0.092282	0.2622		0.089802	0.2533	
	50	0.092285	0.2922		0.089805	0.2804	
		0.092281	0.2480	-1.248	0.089801	0.2405	-1.124
	70	0.092294	0.3257		0.089812	0.3106	
		0.092283	0.2615	-0.934	0.089803	0.2525	-0.847
	90	0.092307	0.3571		0.089825	0.3393	
		0.092286	0.2812	-0.672	0.089806	0.2700	-0.614
	110	0.092326	0.3842		0.089842	0.3642	
		0.092293	0.3038	-0.478	0.089811	0.2904	-0.439
	0.092283	0.2625	-0.91	0.089805	0.2570	-0.82	
Exp. ^c	0.092315(3)	0.2450(73)	$-0.97(35)$	0.089837(4)	0.2370(82)	$-0.97(65)$	
$(1,0^0,1)$	10	0.091805	0.4507		0.089342	0.4268	
	30	0.091805	0.4518		0.089342	0.4279	
	50	0.091805	0.4537		0.089343	0.4294	
	70	0.091805	0.4556		0.089343	0.4310	
		0.091805	0.4522	-0.049	0.089343	0.4282	-0.040
	90	0.091806	0.4564		0.089343	0.4315	
		0.091805	0.4551	-0.011	0.089343	0.4309	-0.005
	110	0.091804	0.4542		0.089342	0.4293	
		0.091807	0.4621	0.047	0.089345	0.4372	0.047
	^e Exp. ^c	0.091806	0.4558		0.0893453	0.4337	
Exp. ^c	0.091848(2)	0.4472(3)		0.0893885(2)	0.4283(5)		

^a Computed band origins: $\nu_3 = 722.90 \text{ cm}^{-1}$ and $\nu_1 + \nu_3 = 983.12 \text{ cm}^{-1}$. ^b Computed band origins: $\nu_3 = 722.96 \text{ cm}^{-1}$ and $\nu_1 + \nu_3 = 979.76 \text{ cm}^{-1}$.

^c Values in parentheses denote one standard deviation and apply to the last digits of the constants. ^d Employing the same sort of fit as in the previous experimental paper (*ref.* 4). ^e Employing the same sort of fit as in the present experimental part (*see* Section 2).

As was mentioned earlier,⁵ such an increase cannot occur within the harmonic approximation and must be due to anharmonicity. The unusual isotope effect is twice as large for $^{37}\text{ClH}^{37}\text{Cl}^-$. The still unknown experimental value for the band origin of that isotopologue is thus predicted to be $\nu_3 (^{37}\text{ClH}^{37}\text{Cl}^-) = 723.02 \text{ cm}^{-1}$. The corresponding rotational and centrifugal distortion constants are calculated to be $B_{001} = 0.08732 \text{ cm}^{-1}$, $D_{001} = 0.243 \times 10^{-7} \text{ cm}^{-1}$, and $H_{001} = -0.77 \times 10^{-12} \text{ cm}^{-1}$, obtained through a least-squares fit to rovibrational energies up to $J_{\text{max}} = 70$. The ground-state values of $^{37}\text{ClH}^{37}\text{Cl}^-$ are predicted to be $B_{000} = 0.09211 \text{ cm}^{-1}$ and $D_{000} = 0.356 \times 10^{-7} \text{ cm}^{-1}$. For the combination vibrational state $(1,0^0,1)$ we obtain $B_{101} = 0.08688 \text{ cm}^{-1}$ and $D_{101} = 0.404 \times 10^{-7} \text{ cm}^{-1}$, again with very stable results for fits with J_{max} up to 110.

Compared to experiment, the calculated band origins of the $\nu_1 + \nu_3$ bands of $^{35}\text{ClH}^{35}\text{Cl}^-$ and $^{37}\text{ClH}^{35}\text{Cl}^-$ are underestimated by 0.14 and 0.15 cm^{-1} , respectively. For $^{37}\text{ClH}^{37}\text{Cl}^-$, we calculate $\nu_1 + \nu_3 = 976.36 \text{ cm}^{-1}$ and, assuming an error of -0.16 cm^{-1} , we would like to make the prediction $\nu_1 + \nu_3 (^{37}\text{ClH}^{37}\text{Cl}^-) = 976.52 \pm 0.02 \text{ cm}^{-1}$.

Predictions for the stretching vibrational states of the overtone series $n\nu_1$ ($n = 1-4$) are made in Table 4. All the four states of the three isotopologues considered appear to be essentially unperturbed up to high J values and therefore three spectroscopic constants (G_v , B_v , and D_v) were determined by a least-squares fit to rotational levels up to $J_{\text{max}} = 30$. Regarding the small errors obtained for the $\nu_1 + \nu_3$ combination tones of $^{35}\text{ClH}^{35}\text{Cl}^-$ and $^{37}\text{ClH}^{35}\text{Cl}^-$, we are confident that the errors in the ν_1 fundamentals will be smaller than 0.2 cm^{-1} and those for the overtones up to $4\nu_1$ should not exceed 1 cm^{-1} . Since the wavenumbers for the $\nu_1 + \nu_3$ bands are underestimated, we may expect that the wavenumbers of the $n\nu_1$ series are slightly too small, as well. For $^{35}\text{ClH}^{35}\text{Cl}^-$, the change in rotational constant upon excitation of the totally symmetric Cl-Cl stretching vibration by 1-4 quanta is predicted to be -0.59% , -1.31% , -2.26% , and -3.42% . Much larger changes are calculated for the quartic centrifugal constant, which increases by 6.9% , 18.6% , 36.4% , and 56.6% .

4.3 Vibrational states $(0,1^1,0)$ and $(1,1^1,0)$ of H isotopologues

In the previous experimental work,⁴ approximate information about the proton bending vibration ν_2 of $^{35}\text{ClH}^{35}\text{Cl}^-$ was obtained through a two-state Coriolis interaction model involving vibrational states $(0,0^0,1)$ and $(0,1^1,0)$. That model is adequate for the case of Coriolis resonance, but may be less suitable for the case of weaker Coriolis interaction. In addition,

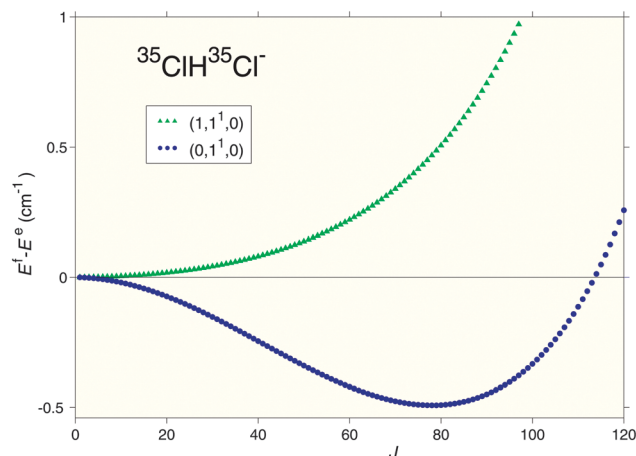


Fig. 4 Calculated splitting between f and e sublevels of $^{35}\text{ClH}^{35}\text{Cl}^-$ in the $(0,1^1,0)$ and $(1,1^1,0)$ vibrational states.

a guess had to be made for the Coriolis coupling constant η in order to arrive at an estimate of $\nu_2 = 792 \pm 9 \text{ cm}^{-1}$. Published values from *ab initio* calculations involving vibrational anharmonicity are 787.3 cm^{-1} (PES I) and 789.1 cm^{-1} (PES II) as obtained by Špirko *et al.*⁸ and 799.1 cm^{-1} as computed by Sebald,¹⁴ all in agreement with Kawaguchi's estimate.

Using the complete Watson Hamiltonian³⁴ and the PES from Section 3, rovibrational term energies have been calculated for the $l = 1$ states $(0,1^1,0)$ and $(1,1^1,0)$ of $^{35}\text{ClH}^{35}\text{Cl}^-$ up to $J_{\text{max}} = 120$ (see ESI† Table S4). As is well known, the rotational levels within such states are split apart by Coriolis coupling and thus exhibit l -type doubling.⁴⁰ The resulting pairs of sublevels have parity $+(-1)^J$ for the e sublevels and $-(-1)^J$ for the f sublevels.⁴¹ The energy differences between f and the corresponding e sublevels of the $(0,1^1,0)$ and $(1,1^1,0)$ states are plotted in Fig. 4. As was already discussed in detail by Sebald,¹⁴ the f sublevels of the $(0,1^1,0)$ state are below the corresponding e sublevels up to high values of J , leading to negative values of the energy difference $\Delta E(J) = E^f(J) - E^e(J)$ in that range. According to the present calculations, the graph of the function $\Delta E(J)$ has a minimum at $J = 78$ and $\Delta E(J)$ changes sign between $J = 113$ and $J = 114$. Such a change of $\Delta E(J)$ appears to be rather unusual and results from anharmonic interaction with other vibrational states, to be discussed in more detail in Section 4.4. On the other hand, and perhaps surprisingly, the graph of $\Delta E(J)$ for the combination vibrational state $(1,1^1,0)$ shows a rather normal shape, with monotonically rising positive values over the whole range of J values being considered.

Table 4 Effective spectroscopic constants of the $n\nu_1$ overtone series of $^{35}\text{ClH}^{35}\text{Cl}^-$, $^{37}\text{ClH}^{35}\text{Cl}^-$, and $^{37}\text{ClH}^{37}\text{Cl}^-$ (in cm^{-1})^a

Vibrational state	$^{35}\text{ClH}^{35}\text{Cl}^-$			$^{37}\text{ClH}^{35}\text{Cl}^-$			$^{37}\text{ClH}^{37}\text{Cl}^-$		
	G_v	B_v	$D_v (\times 10^7)$	G_v	B_v	$D_v (\times 10^7)$	G_v	B_v	$D_v (\times 10^7)$
$(1,0^0,0)$	302.76	0.096800	0.4250	298.74	0.094197	0.4016	294.66	0.091594	0.3791
$(2,0^0,0)$	597.31	0.096091	0.4713	589.54	0.093522	0.4441	581.66	0.090950	0.4184
$(3,0^0,0)$	880.84	0.095177	0.5423	869.73	0.092656	0.5090	858.45	0.090127	0.4784
$(4,0^0,0)$	1150.39	0.094037	0.6226	1136.45	0.091589	0.6104	1122.28	0.089100	0.5488

^a Obtained from fits with $J_{\text{max}} = 30$.

Table 5 Calculated effective spectroscopic constants (in cm^{-1}) for the $(0,1^1,0)$ and $(1,1^1,0)$ states of $^{35}\text{ClH}^{35}\text{Cl}^-$ ^a

State	J_{max}	G_v	B_v	$D_v (\times 10^7)$	$q_v (\times 10^3)$	$q_D (\times 10^7)$
$(0,1^1,0)$	10	795.75	0.098133	0.5442	-0.184	0.23
	30	795.75	0.098133	0.5356	-0.184	0.22
	50	795.75	0.098131	0.5224	-0.181	0.19
	70	795.75	0.098128	0.5088	-0.173	0.16
	90	795.75	0.098123	0.4977	-0.163	0.14
	110	795.76	0.098119	0.4917	-0.152	0.12
$(1,1^1,0)$	10	1090.33	0.097381	0.4942	0.040	0.05
	30	1090.33	0.097381	0.4949	0.040	0.05
	50	1090.33	0.097381	0.4967	0.040	0.06
	70	1090.33	0.097382	0.5003	0.039	0.06
	90	1090.33	0.097385	0.5071	0.035	0.07
	110	1090.33	0.097394	0.5205	0.022	0.09

^a See eqn (7) and (8) for definition.

In order to deduce effective spectroscopic constants for the states $(0,1^1,0)$ and $(1,1^1,0)$, we have fitted the energies of their e and f sublevels with the formulae

$$\frac{E^f + E^e}{2} = G_v + B_v[J(J+1) - 1] - D_v[J(J+1) - 1]^2 \quad (7)$$

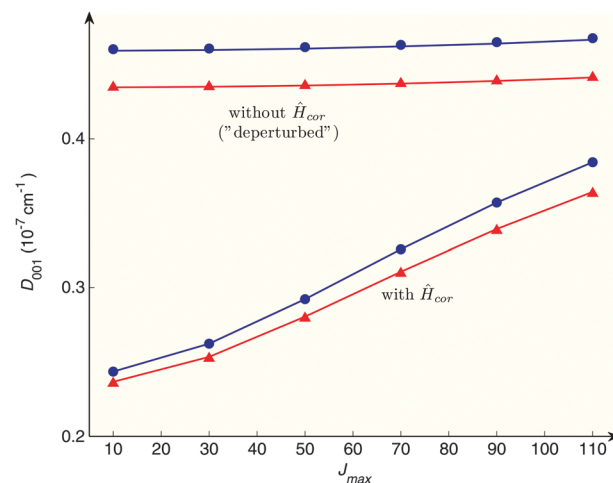
$$E^f - E^e = q_v J(J+1) + q_D [J(J+1)]^2 \quad (8)$$

Results of the fits are given in Table 5. Six different values of J_{max} were considered. Whereas G_{010} and B_{010} are almost independent of J_{max} , the corresponding centrifugal distortion constant and the l -type doubling constants (q_v and q_D) show significant variation which may be indicative of Coriolis coupling with other states. In particular, the q_D value of the $(0,1^1,0)$ state as calculated with $J_{\text{max}} = 110$ is only about half as large as the value obtained with $J_{\text{max}} = 10$. The l -type doubling constant q_v has a negative sign, meaning that the e levels are shifted upward by Coriolis interaction, as expected for the upper state of the interacting pair $(0,0^0,1)/(0,1^1,0)$.

For the $(1,1^1,0)$ state, the situation is quite different compared with the $(0,1^1,0)$ state, all spectroscopic constants being rather insensitive with respect to variation of J_{max} up to $J_{\text{max}} = 90$. As is obvious from the shape of the graph shown in Fig. 4, both l -type doubling constants (q_v and q_D) have the same sign. Predictions for the $(0,1^1,0)$ and $(1,1^1,0)$ states of $^{37}\text{ClH}^{35}\text{Cl}^-$ and $^{37}\text{ClH}^{37}\text{Cl}^-$ are provided in the ESI† (Table S5).

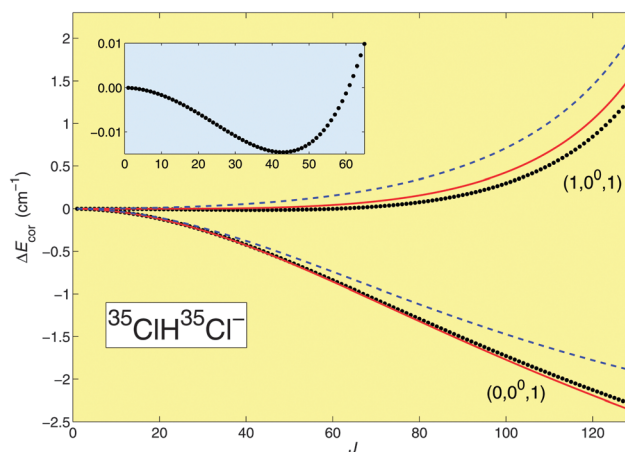
4.4 Analysis of Coriolis interaction between low-lying vibrational states of $^{35}\text{ClH}^{35}\text{Cl}^-$

In order to analyse the effects of Coriolis interaction between different vibrational states, we have compared the results of rovibrational calculations with and without inclusion of \hat{H}_{cor} in the rovibrational Hamiltonian. For the vibrational ground state, the differences in rovibrational term energies (termed $\Delta E_{\text{cor}}(J)$) are extremely small and do not exceed 0.015 cm^{-1} for J values smaller than 110. Consequently, the effect of neglecting \hat{H}_{cor} on the rotational and centrifugal distortion constants of this state is negligibly small. For the $(0,0^0,1)$ states of $^{35}\text{ClH}^{35}\text{Cl}^-$ and of $^{37}\text{ClH}^{35}\text{Cl}^-$, the situation is quite different (see Fig. 5).

**Fig. 5** Dependence of effective and "deperturbed" quartic centrifugal distortion constants on J_{max} for $^{35}\text{ClH}^{35}\text{Cl}^-$ (filled circles) and $^{37}\text{ClH}^{35}\text{Cl}^-$ (triangles).

Neglecting \hat{H}_{cor} , all rovibrational states up to $J_{\text{max}} = 110$ are fitted very well without inclusion of the H_{001} term, and the resulting deperturbed D_{001} values vary only slightly between 0.4591×10^{-7} and $0.4665 \times 10^{-7} \text{ cm}^{-1}$ for $^{35}\text{ClH}^{35}\text{Cl}^-$ and between 0.4345×10^{-7} and $0.4411 \times 10^{-7} \text{ cm}^{-1}$ for $^{37}\text{ClH}^{35}\text{Cl}^-$. The values obtained for the former isotopologue agree nicely with the experimental result of $0.4528(61) \times 10^{-7} \text{ cm}^{-1}$ as obtained from Kawaguchi's earlier analysis.⁴ Good agreement is also observed with the earlier theoretical values of Špirko *et al.*⁸ (0.42×10^{-7} and $0.46 \times 10^{-7} \text{ cm}^{-1}$ from PES I and II, respectively). As is already known from the results of Table 3, the effective D_{001} values displayed in the lower part of Fig. 5 increase strongly with J_{max} . For the $(1,0^0,1)$ states of $^{35}\text{ClH}^{35}\text{Cl}^-$ and of $^{37}\text{ClH}^{35}\text{Cl}^-$, the ratios between effective and deperturbed quartic centrifugal distortion constants depend only slightly on J_{max} , varying in the small range between 0.901 and 0.917. Coriolis interaction thus lowers the D_{101} values by less than 10%.

The graphs of $\Delta E_{\text{cor}}(J)$ for the stretching vibrational states $(0,0^0,1)$ and $(1,0^0,1)$ are displayed in Fig. 6 (filled black circles).

**Fig. 6** Contribution of Coriolis interaction to the rovibrational energies of states $(0,0^0,1)$ and $(1,0^0,1)$ for $^{35}\text{ClH}^{35}\text{Cl}^-$ (for details see the text).

Not surprisingly, and mainly as a result of Coriolis interaction with the higher-lying state $(0,1^1,0)$, the graph of function $\Delta E_{\text{cor}}(J)$ for the $(0,0^0,1)$ state has a monotonically decreasing shape. For the $(1,0^0,1)$ state, the situation is rather different. Over the wide range up to about $J = 60$, its graph is almost a horizontal line, with tiny negative values, and then rises rather steeply. In order to rationalize that behaviour and to get more insight into the relevant Coriolis interaction, we have set up a number of model calculations involving a small number of interacting vibrational states. In an obvious shorthand notation including energetic numbering in ascending order (in parentheses), these are 001(1), 010(2), 101(3), 110(4), and 210(5). Direct Coriolis interaction of states $(0,0^0,1)$ and $(1,0^0,1)$ occurs with states of type $(\nu_1,1^1,0)$. For a given value of J , the chosen model Hamiltonian has the following form:

$$H_{\text{model}}(J) = \begin{pmatrix} E_{001}(J) & & & & & \text{sym.} \\ \in_{21} X & E_{010}(J) & & & & \\ 0 & \in_{32} X & E_{101}(J) & & & \\ \in_{41} X & 0 & \in_{43} X & E_{110}(J) & & \\ \in_{51} X & 0 & \in_{53} X & 0 & E_{210}(J) & \end{pmatrix}$$

with $X = \sqrt{J(J+1)}$

(9)

The J -dependent diagonal elements of the model Hamiltonian are obtained as eigenvalues of $\hat{H} - \hat{H}_{\text{cor}}$ (see eqn (5)), whereas the non-vanishing off-diagonal elements are chosen of the form $\in_{ij} \sqrt{J(J+1)}$. Here, the parameters \in_{ij} are calculated as matrix elements of \hat{H}_{cor} over the rovibrational eigenfunctions of $\hat{H} - \hat{H}_{\text{cor}}$ for $J = 1$. According to the present calculations, the matrix elements of $\hat{H} - \hat{H}_{\text{cor}}$ are almost independent of J and thus the use of constant values is justified well. *E.g.*, we compute $\in_{21}(J = 1) = 0.1376 \text{ cm}^{-1}$ and $\in_{21}(J = 120) = 0.1292 \text{ cm}^{-1}$. For $^{35}\text{ClH}^{35}\text{Cl}^-$, the numerical values chosen for the interaction parameters are (in cm^{-1}): $\in_{21} = 0.1376$, $\in_{41} = 0.1021$, $\in_{51} = -0.0485$, $\in_{32} = -0.1066$, $\in_{43} = 0.0589$, and $\in_{53} = -0.1101$.

Results of the model calculations as obtained by diagonalizing H_{model} for different values of J are included in Fig. 6. The functions $\Delta E_{\text{cor}}(J)$ are defined only pointwise, but for better visibility we have partly chosen them to be continuous functions. Very good agreement with the variational calculations is obtained by the full model with five states and six non-vanishing off-diagonal matrix elements (full red lines). A reduced two-state model for the proton stretching vibrational state, involving states 001 and 010 (dashed blue line in lower part of Fig. 6), works reasonably well for low values of J , but deviates significantly from the variational results for $J > 50$.

The upper state $(1,0^0,1)$ considered in Fig. 6 is shifted upward through direct Coriolis interaction with state 010 and downward through interaction with state 110. A minimum of these three states (see dashed blue line in the upper part of Fig. 6) is thus required to obtain a qualitatively correct form

of $\Delta E_{\text{cor}}(J)$. Owing to the rather large value of \in_{53} , interaction with state 210 is also significant.

The model Hamiltonian was also employed to study the J dependence of the f-e splitting in the $(0,1^1,0)$ state of $^{35}\text{ClH}^{35}\text{Cl}^-$ (see ESI† Fig. S1). A two-state model involving states 010 and 001 is clearly inadequate to properly describe the J dependence of that splitting for $J > 20$. The situation is much improved by inclusion of state 101, and almost quantitative agreement with the full variational calculations is obtained for a four-state model in which state 201 is added to the three-state model.

4.5 Predictions for deuterated isotopologues

High-resolution IR studies for deuterated isotopologues of the hydrogen bichloride ion are not yet available and so theory may provide useful predictions. For this purpose, we have carried out variational calculations of rovibrational states and transition dipole moments among them on the basis of the analytical PEFs and EDMFs discussed earlier, the latter being modified appropriately to account for the change in nuclidic masses. The most important results are presented in a compact manner in Table 6, which comprises spectroscopic constants for the vibrational ground state, the three singly-excited vibrational states and the doubly excited states $(1,0^0,1)$ and $(1,1^1,0)$. In the case of the states with $l = 1$, the l -type doubling constants q_v and q_D are quoted as well. Details of the fitting procedures employed to determine the spectroscopic constants are given in the footnotes to the table.

Upon deuterium substitution, the symmetric stretching vibration ν_1 experiences a slight increase in wavenumber, ranging between 1.76 cm^{-1} for $^{35}\text{ClD}^{35}\text{Cl}^-$ and 1.82 cm^{-1} for $^{37}\text{ClD}^{37}\text{Cl}^-$. Such an increase is not allowed within the harmonic approximation and must be the result of the anharmonic nature of the potential energy surface. The origins of the ν_3 bands of the deuterated species $^{35}\text{ClD}^{35}\text{Cl}^-$ and $^{37}\text{ClD}^{35}\text{Cl}^-$, and $^{37}\text{ClD}^{37}\text{Cl}^-$ are predicted at 483.92 , 483.88 , and 483.84 cm^{-1} , with an estimated accuracy of better than 1 cm^{-1} . In contrast to the H isotopologues, no unusual effects are predicted upon ^{37}Cl substitution. A neon matrix-isolation IR spectroscopic study by Forney *et al.*²⁰ reported absorptions at 489.3 and 496.2 cm^{-1} , both of which were attributed to ClDCl^- . Like for the most abundant isotopologue, the neon matrix environment produces a slight blue shift in the antisymmetric stretching vibration. The earlier argon-matrix studies²¹ yielded $\nu_3(\text{ClDCl}^-) = 463 \text{ cm}^{-1}$ and thus a red-shift of 21 cm^{-1} with respect to the present prediction. While no neon-matrix value is available for the combination tone $\nu_1 + \nu_3(\text{ClDCl}^-)$, a weak, relatively broad absorption at 730 cm^{-1} observed in an argon matrix was assigned to that band.²¹ It also exhibits a red-shift of 21 cm^{-1} with respect to our theoretical value (Table 6).

The deuteron bending vibrational energy of $^{35}\text{ClD}^{35}\text{Cl}^-$ is predicted to be $G_{010} = 571.32 \text{ cm}^{-1}$, with an uncertainty of *ca.* 1 cm^{-1} . Again, the energy is higher than that of the deuteron stretching vibration ($G_{001} = 483.92 \text{ cm}^{-1}$), the difference of 87.40 cm^{-1} being even larger than in the case of $^{35}\text{ClH}^{35}\text{Cl}^-$ (72.85 cm^{-1}). Consequently, the l -type doubling constant q_v again has a negative value.

Table 6 Predicted effective spectroscopic constants (in cm^{-1}) for deuterated isotopologues^a

Isotopologue	State	G_v	B_v	D_v	$q_v (\times 10^3)$	$q_D (\times 10^7)$
³⁵ ClD ³⁵ Cl ⁻	(0,0 ⁰ ,0)	989.49 ^b	0.097724	0.3940		
	(1,0 ⁰ ,0)	304.52	0.097056	0.4389		
	(0,0 ⁰ ,1) ^c	483.92	0.093706	0.2934		
	(0,1 ¹ ,0)	571.32	0.098330	0.4988	-0.231	0.16
	(1,0 ⁰ ,1)	750.77	0.093076	0.4424		
	(1,1 ¹ ,0)	868.74	0.097467	0.5163	-0.018	0.07
³⁷ ClD ³⁵ Cl ⁻	(0,0 ⁰ ,0)	986.98 ^b	0.095086	0.3728		
	(1,0 ⁰ ,0)	300.53	0.094447	0.4144		
	(0,0 ⁰ ,1) ^d	483.88	0.091187	0.2821		
	(0,1 ¹ ,0)	571.13	0.095671	0.4701	-0.216	0.15
	(1,0 ⁰ ,1)	747.27	0.090583	0.4190		
	(1,1 ¹ ,0)	864.69	0.094847	0.4868	-0.014	0.07
³⁷ ClD ³⁷ Cl ⁻	(0,0 ⁰ ,0)	984.45 ^b	0.092452	0.3523		
	(1,0 ⁰ ,0)	296.48	0.091842	0.3906		
	(0,0 ⁰ ,1) ^e	483.84	0.088671	0.2707		
	(0,1 ¹ ,0)	570.95	0.093016	0.4424	-0.202	0.14
	(1,0 ⁰ ,1)	743.73	0.088093	0.3963		
	(1,1 ¹ ,0)	860.59	0.092231	0.4581	-0.010	0.06

^a Obtained by least-squares fit to rovibrational energies up to $J_{\text{max}} = 30$. ^b Zero-point energy. ^c $H_{001} = -0.819 \times 10^{-12} \text{ cm}^{-1}$. ^d $H_{001} = -0.733 \times 10^{-12} \text{ cm}^{-1}$. ^e $H_{001} = -0.654 \times 10^{-12} \text{ cm}^{-1}$.

As was already found in the calculations by Špirko *et al.*,⁸ deuterium substitution leads to an increase in the rotational constant B_{000} . For ³⁵ClD³⁵Cl⁻, we calculate $\Delta B_{000} = 0.000357 \text{ cm}^{-1}$, in excellent agreement with the previous prediction of 0.00037 cm^{-1} .⁸ The increase is still more pronounced for B_{001} and B_{101} , where differences of 0.001424 and 0.001271 cm^{-1} are obtained. On the other hand, B_{010} (³⁵ClD³⁵Cl⁻) exceeds B_{010} (³⁵ClH³⁵Cl⁻) by only 0.000197 cm^{-1} , smaller than the difference for the vibrational ground state.

4.6 Transition dipole moments

Squares of transition dipole moments for two series of vibrational transitions of ³⁵ClH³⁵Cl⁻ and ³⁵ClD³⁵Cl⁻ are listed in Table 7. The first series arises from the vibrational ground state, while the second one corresponds to hot transitions starting from the first excited state of the symmetric stretching vibration with energies of 303 cm^{-1} (³⁵ClH³⁵Cl⁻) and 305 cm^{-1} (³⁵ClD³⁵Cl⁻) above the vibrational ground-state. As expected, the largest μ^2 values are obtained for the ν_3 bands. The present values of 2.011 D^2 and 1.942 D^2 are only slightly larger than the results of the earlier CEPA calculations (1.777 and 1.793 D^2).⁵ Among the transitions considered in Table 7, only two of them are allowed within the familiar double-harmonic approximation (DHA). These are the fundamental transition $(0,0^0,1) \leftarrow (0,0^0,0)$ and the hot band $(1,0^0,1) \leftarrow (1,0^0,0)$. Actually, it is mechanical anharmonicity arising from the strongly anharmonic nature of the PES, consideration of which is decisive to arrive at accurate values for the transition dipole moments. Including only the linear EDMF term D''_{001} (see ESI† Table S2) in the calculations, μ^2 values for the two transitions are obtained, which differ from those of the full treatment by less than 13%. Interestingly, it is not the DHA-allowed

Table 7 Squares of transition dipole moments $\mu_{v,v'}^2$ (in D^2) for stretching vibrational transitions of ³⁵ClH³⁵Cl⁻ and ³⁵ClD³⁵Cl⁻

Upper state	Lower state	³⁵ ClH ³⁵ Cl ⁻		³⁵ ClD ³⁵ Cl ⁻	
		Full ^a	1-Term ^b	Full ^a	1-Term ^b
(0,0 ⁰ ,1)	(0,0 ⁰ ,0)	2.011	2.262	1.942	2.132
(1,0 ⁰ ,1)		0.664	0.731	0.324	0.344
(2,0 ⁰ ,1)		0.145	0.158	0.044	0.047
(3,0 ⁰ ,1)		0.026	0.028	0.005	0.005
(0,0 ⁰ ,1)	(1,0 ⁰ ,0)	1.488	1.707	1.087	1.222
(1,0 ⁰ ,1)		0.603	0.692	1.147	1.283
(2,0 ⁰ ,1)		0.760	0.840	0.485	0.514
(3,0 ⁰ ,1)		0.313	0.342	0.116	0.123

^a Complete EDMF (see ESI Table S2) is employed. ^b Only the EDMF term D''_{001} is employed.

transition which has the largest μ^2 value of the hot bands of ³⁵ClH³⁵Cl⁻. Instead, a value larger by a factor of 2.5 is calculated for the DHA-forbidden transition $(0,0^0,1) \leftarrow (1,0^0,0)$. The situation is different for ³⁵ClD³⁵Cl⁻, where μ^2 for the DHA-allowed transition (1.147 D^2) is slightly larger than for the noted DHA-forbidden transition. However, again owing to high mechanical anharmonicity, the μ^2 value for the DHA-allowed hot transition in ³⁵ClD³⁵Cl⁻ exceeds the corresponding value for ³⁵ClH³⁵Cl⁻ by a factor of 1.9, which must be considered a rather unusual deuterium effect.

In contrast to FHF⁻ and FDF⁻, where 14 and 22 lines were observed in the ν_2 bands,^{2,3} and relatively large μ^2 values of 0.051 and 0.042 D^2 were calculated recently,⁴² a much smaller value of 0.0050 D^2 was computed for the ν_2 band of ³⁵ClH³⁵Cl⁻. Since Coriolis interaction between the $(0,0^0,1)$ and $(0,1^1,0)$ states of ³⁵ClH³⁵Cl⁻ is much weaker, intensity borrowing is less pronounced for the bichloride ion.

5. Conclusions

High-resolution spectroscopic investigations of hydrogen-bonded anionic complexes are very scarce and essentially limited to the pioneering work of Kawaguchi and Hirota on FHF⁻ and ClHCl⁻.¹⁻⁴ For the less strongly bound species ³⁵ClH³⁵Cl⁻ and ³⁷ClH³⁵Cl⁻, only the ν_3 bands (corresponding to the proton stretching vibrations) were analysed, exhibiting indication of Coriolis interaction with the higher-lying proton bending vibrational state.⁴ With the aid of accompanying high-level quantum chemical calculations, 45 and 41 lines within the $\nu_1 + \nu_3$ combination tones of ³⁵ClH³⁵Cl⁻ and ³⁷ClH³⁵Cl⁻ observed earlier could now be faithfully assigned. The variational calculations of rovibrational energies and wave functions are based on Watson's Hamiltonian for linear molecules³⁴ and an empirically corrected CCSD(T*)-F12b potential energy surface. In contrast to the earlier work on the ν_3 bands,⁴ all lines could be fitted very well with just three parameters (G_v , B_v , and D_v). However, that does not mean that Coriolis interaction plays no role for the $(1,0^0,1)$ vibrational state. Instead, computations with a five-state model Hamiltonian show that more than three interacting states are required to quantitatively describe the variation of the Coriolis contribution to the rovibrational energies within state $(1,0^0,1)$ up to high values of J .

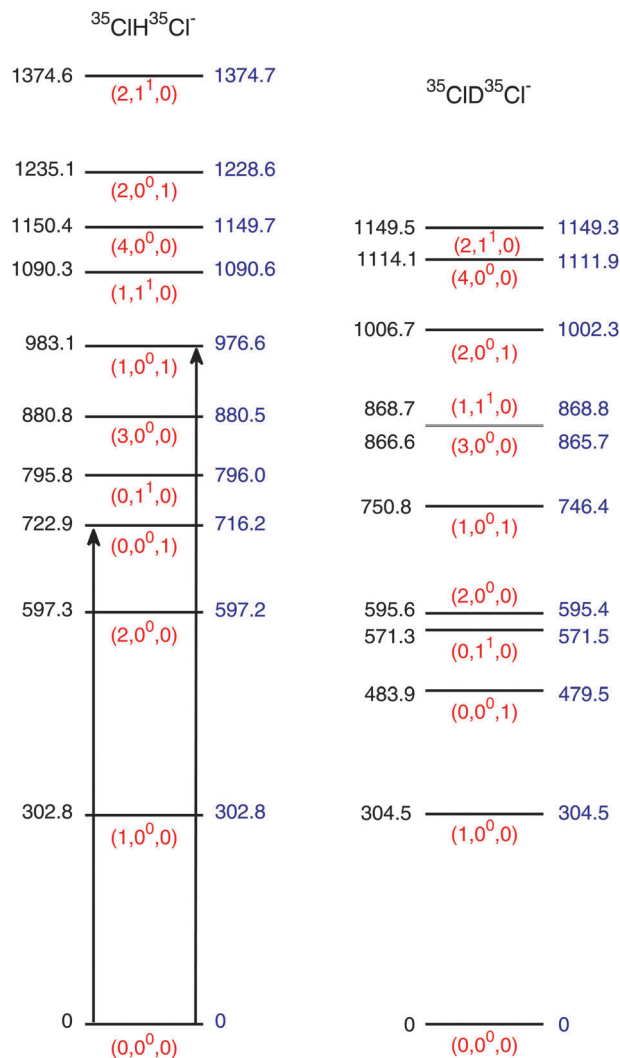


Fig. 7 Calculated term energies (in cm^{-1}) for lowest 11 vibrational states of $^{35}\text{ClH}^{35}\text{Cl}^-$ and $^{35}\text{ClD}^{35}\text{Cl}^-$. Left columns: data obtained with empirically corrected PEF; right columns: data obtained with CCSD(T*)-F12b/AV5Z PEF. Observed transitions are indicated by arrows.

The ν_3 and $\nu_1 + \nu_3$ bands of ClHCl^- isotopologues are characterized by band heads which are a rare issue in rovibrational spectroscopy. For $^{35}\text{ClH}^{35}\text{Cl}^-$ and $^{37}\text{ClH}^{35}\text{Cl}^-$ the heads of the ν_3 bands are calculated at line R(18) with wavenumbers of 724.665 and 724.681 cm^{-1} , respectively. For the combination tone, we predict the band heads to occur at R(16) with wavenumbers of 984.729 and 981.333 cm^{-1} .

According to the present calculations, the Coriolis interaction between states $(0,0,1)$ and $(0,1,0)$ is relatively weak such that no significant intensity borrowing takes place and no line within the ν_2 band could be observed so far. Our calculations predict $G_{010} = 795.75 \text{ cm}^{-1}$, with an uncertainty of ca. 1 cm^{-1} . We thus support Kawaguchi's earlier estimate of $792 \pm 9 \text{ cm}^{-1}$,⁴ which was based on a two-state model and an educated guess of the Coriolis coupling constant η .

Finally, Fig. 7 presents an overview of the 11 vibrational states of $^{35}\text{ClH}^{35}\text{Cl}^-$ and $^{35}\text{ClD}^{35}\text{Cl}^-$ which we have investigated

in the present work, including their calculated vibrational energies. The two arrows indicate the transitions which have been observed by Kawaguchi.⁴ The figure includes data from calculations with both empirically corrected and uncorrected PEFs. The latter differ from experiment by 6.7 cm^{-1} for both ν_3 and $\nu_1 + \nu_3$. Most of the error in the CCSD(T*)-F12b calculations probably results from the neglect of core valence (CV) correlation and scalar relativistic effects. We have investigated the former by means of standard CCSD(T)¹⁰ in conjunction with the ACVQZ basis set, whereas the latter were studied within the Douglas–Kroll–Hess (DKH) approximation of 2nd order^{43,44} using the AVTZ basis set. Inclusion of CV correlation increases ν_3 by 4.5 cm^{-1} and the DKH correction amounts to +4.7 cm^{-1} . Adding the sum to the uncorrected ν_3 value, we arrive at 725.8 cm^{-1} and thus at an overestimate by 2.9 cm^{-1} . The latter difference with respect to experiment is attributed to the neglect of higher-order correlation effects (in particular quadruple substitutions) and potentially Born–Oppenheimer breakdown contributions. The explicit consideration of higher-order correlation contributions would be very expensive for ClHCl^- , since time-consuming calculations at many different nuclear configurations would have to be carried out.

The information of Fig. 7 may be helpful to forthcoming spectroscopic work on the bichloride system. In particular, assignments of lines within the hot band $(1,0,1) \leftarrow (1,0,0)$ would be of great interest since it would open the way to a precise determination of the ν_1 band origin. Unfortunately, the μ^2 value for that band is relatively low (see Table 7) and the situation appears to be less favorable than for FHF^- where the corresponding transition was observed earlier.² Extension of the previous spectroscopic work to a transition to the first overtone of the proton stretching vibration $(0,0,2)$ appears to be of interest as well. For $^{35}\text{ClH}^{35}\text{Cl}^-$, its vibrational term value is predicted at 1746.3 cm^{-1} , with effective rotational and quartic centrifugal distortion constants of 0.09339 cm^{-1} and $0.270 \times 10^{-7} \text{ cm}^{-1}$ from fits with $J_{\text{max}} = 70$, respectively. According to our calculations, observation might be possible in the form of a hot band with initial state $(0,0,1)$, the band origin being predicted at 1023.4 cm^{-1} and the transition dipole moment calculated to be 1.429 D.

References

- 1 K. Kawaguchi and E. Hirota, *J. Chem. Phys.*, 1986, **84**, 2953.
- 2 K. Kawaguchi and E. Hirota, *J. Chem. Phys.*, 1987, **87**, 6838.
- 3 K. Kawaguchi and E. Hirota, *J. Mol. Struct.*, 1995, **352/353**, 389.
- 4 K. Kawaguchi, *J. Chem. Phys.*, 1988, **88**, 4186.
- 5 P. Botschwina, P. Sebald and R. Burmeister, *J. Chem. Phys.*, 1988, **88**, 5246.
- 6 W. Meyer, *J. Chem. Phys.*, 1973, **58**, 1017.
- 7 S. Ikuta, T. Saitoh and O. Nomura, *J. Chem. Phys.*, 1989, **91**, 3539.
- 8 V. Špirko, A. Čejchan and G. H. F. Dierksen, *Chem. Phys.*, 1991, **151**, 45.

- 9 J. E. Del Bene and M. J. T. Jordan, *Spectrochim. Acta, Part A*, 1999, **55**, 719.
- 10 K. Raghavachari, G. W. Trucks, J. A. Pople and M. Head-Gordon, *Chem. Phys. Lett.*, 1989, **157**, 479.
- 11 T. H. Dunning, Jr., *J. Chem. Phys.*, 1989, **90**, 1007.
- 12 R. A. Kendall, T. H. Dunning, Jr. and R. J. Harrison, *J. Chem. Phys.*, 1992, **96**, 6796.
- 13 D. E. Woon and T. H. Dunning, Jr., *J. Chem. Phys.*, 1993, **98**, 1358.
- 14 P. Sebald, *Chem. Phys.*, 2008, **346**, 77.
- 15 H.-J. Werner, T. B. Adler, G. Knizia and F. R. Manby, in *Recent Progress in Coupled Cluster Methods: Theory and Applications*, ed. P. Carsky, J. Pitter and J. Paldus, Springer, 2010.
- 16 D. P. Tew, C. Hättig, R. A. Bachorz and W. Klopper, in *Recent Progress in Coupled Cluster Methods: Theory and Applications*, ed. P. Carsky, J. Pitter and J. Paldus, Springer, 2010.
- 17 C. Hättig, W. Klopper, A. Köhn and D. P. Tew, *Chem. Rev.*, 2012, **112**, 4.
- 18 L. Kong, F. A. Bischoff and E. F. Valeev, *Chem. Rev.*, 2012, **112**, 75.
- 19 K. Kawaguchi, C. Yamada, S. Saito and E. Hirota, *J. Chem. Phys.*, 1985, **82**, 1750.
- 20 D. Forney, M. E. Jacox and W. E. Thompson, *J. Chem. Phys.*, 1995, **103**, 1755.
- 21 D. E. Milligan and M. E. Jacox, *J. Chem. Phys.*, 1970, **53**, 2034.
- 22 T. B. Adler, G. Knizia and H.-J. Werner, *J. Chem. Phys.*, 2007, **127**, 221106.
- 23 G. Knizia, T. B. Adler and H.-J. Werner, *J. Chem. Phys.*, 2009, **130**, 054104.
- 24 H.-J. Werner, G. Knizia, T. B. Adler and O. Marchetti, *Z. Phys. Chem.*, 2010, **224**, 493.
- 25 T. H. Dunning, Jr., K. A. Peterson and A. K. Wilson, *J. Chem. Phys.*, 2001, **114**, 9244 and references therein.
- 26 K. E. Yousaf and K. A. Peterson, *Chem. Phys. Lett.*, 2009, **476**, 303.
- 27 F. Weigend, *Phys. Chem. Chem. Phys.*, 2002, **4**, 4285.
- 28 C. Hättig, *Phys. Chem. Chem. Phys.*, 2005, **7**, 59.
- 29 K. A. Peterson, T. B. Adler and H.-J. Werner, *J. Chem. Phys.*, 2008, **128**, 084102.
- 30 H.-J. Werner, P. J. Knowles, R. Lindh, F. R. Manby and M. Schütz, *et al.*, *MOLPRO version 2009.1, a package of ab initio programs*, 2009, see <http://www.molpro.net>.
- 31 P. Botschwina, P. Sebald, D. Figgen and H. Stoll, *Mol. Phys.*, 2007, **105**, 1193.
- 32 P. Sebald, R. Oswald, P. Botschwina, H. Stoll and D. Figgen, *J. Phys. Chem. A*, 2009, **113**, 11772.
- 33 P. Sebald, H. Vennekate, R. Oswald, P. Botschwina and H. Stoll, *Mol. Phys.*, 2010, **108**, 487.
- 34 J. K. G. Watson, *Mol. Phys.*, 1970, **19**, 465.
- 35 R. J. Whitehead and N. C. Handy, *J. Mol. Spectrosc.*, 1975, **55**, 356.
- 36 R. N. Zare, *Angular Momentum*, John Wiley & Sons Inc, New York, 1988.
- 37 S. Carter, J. Senekowitsch, N. C. Handy and P. Rosmus, *Mol. Phys.*, 1987, **65**, 143.
- 38 R. Herman and R. F. Wallis, *J. Chem. Phys.*, 1955, **23**, 637.
- 39 J. K. G. Watson, *J. Mol. Spectrosc.*, 1987, **125**, 428.
- 40 J. K. G. Watson, *Can. J. Phys.*, 2001, **79**, 521 and references therein.
- 41 J. M. Brown, J. T. Hougen, K.-P. Huber, J. W. C. Johns, I. Kopp, H. Lefebvre-Brion, A. J. Merer, D. A. Ramsey, J. Rostas and R. N. Zare, *J. Mol. Spectrosc.*, 1975, **55**, 500.
- 42 P. Sebald, A. Bargholz, R. Oswald, C. Stein and P. Botschwina, *J. Phys. Chem. A*, DOI: 10.1021/jp3123677.
- 43 M. Douglas and N. M. Kroll, *Ann. Phys.*, 1974, **82**, 89.
- 44 G. Jansen and B. A. Hess, *Phys. Rev. A: At., Mol., Opt. Phys.*, 1989, **39**, 6016.